

Uniwersytet Jagielloński w Krakowie
Wydział Fizyki, Astronomii i Informatyki Stosowanej

Julia Agnieszka Gnatek

Nr albumu: 1100752

**Plastic scintillators as an alternative for
crystals in PET - determination of the
counting efficiency**

Praca licencjacka
na kierunku Biofizyka

Praca wykonana pod kierunkiem
dr. Eryka Czerwińskiego
Instytut Fizyki
Zakład Fizyki Jądrowej

Kraków, 2017

Oświadczenie autora pracy

Świadoma odpowiedzialności prawnej oświadczam, że niniejsza praca dyplomowa została napisana przeze mnie samodzielnie i nie zawiera treści uzyskanych w sposób niezgodny z obowiązującymi przepisami.

Oświadczam również, że przedstawiona praca nie była wcześniej przedmiotem procedur związanych z uzyskaniem tytułu zawodowego w wyższej uczelni.

Kraków, dnia

Podpis autora pracy

Oświadczenie kierującego pracą

Potwierdzam, że niniejsza praca została przygotowana pod moim kierunkiem i kwalifikuje się do przedstawienia jej w postępowaniu o nadanie tytułu zawodowego.

Kraków, dnia

Podpis kierującego pracą

Abstract

The aim of this work was to experimentally check the theoretical predictions of plastic scintillators' efficiency. The BC-420 scintillators have been used in the prototype of the J-PET detector. The measurement system consisted of two BaF₂ detectors, a plastic detector, an oscilloscope, 4 photomultipliers and a sodium isotope ²²Na (as a source of positrons). The assessment of the plastic scintillators' efficiency was conducted by counting the number of registered and unregistered events from 511 keV gamma ray beam.

The efficiency was determined for 6 detector depths, in particular for 1.9 cm, which is the thickness of plastic scintillators used in the J-PET system. The obtained efficiency for this setup is $(11.1 \pm 0.3_{stat} \pm 3.0_{syst})\%$, for events with energy deposited greater than 100 keV, while theoretical prediction is 11.6 % with negligible error.

Abstrakt

Praca ta miała na celu doświadczalne wyznaczenie wydajności zliczeń scyntylatorów plastikowych (BC-420), wykorzystanych w prototypie tomografu J-PET. W doświadczeniu wykorzystano 2 kryształowe detektory BaF₂, scyntylator plastikowy, oscyloskop, 4 fotopowielacze oraz izotop promieniotwórczy ²²Na (jako emiter pozytonów). Wydajność wyznaczono poprzez pomiar liczby zarejestrowanych i niezarejestrowanych kwantów o energii 511 keV przez detektor plastikowy.

Wydajność została wyznaczona doświadczalnie dla 6 różnych grubości scyntylatora, szczególną uwagę zwrócono na wartość 1.9 cm, gdyż odpowiada ona grubości scyntylatorów użytych w tomografie J-PET. Wyniki uzyskane eksperymentalnie wynoszą: $(11.1 \pm 0.3_{stat} \pm 3.0_{syst})\%$, (dla zdarzeń, w których energia zdeponowana przez kwant jest większa od 100 keV), podczas gdy teoretyczna wartość wydajności dla detektora o grubości 1,9 cm wynosi: 11,6 %.

Contents

Abstract	5
Abstrakt	7
Chapter 1 Motivation	11
Chapter 2 Introduction to PET imaging technique	13
Chapter 3 Polymer Scintillators as a novel approach in PET	17
Chapter 4 Efficiency measurements	21
4.1. Experimental setup	21
4.2. Performed measurements	23
4.3. Detectors geometry.....	24
Chapter 5 Data Analysis	25
Chapter 6 Results and Conclusions	29
Bibliography	35

Chapter 1

Motivation

Modern medical diagnostics finds imaging techniques such as positron emission tomography (PET) useful especially as a part of treatment-planning procedure in radiotherapy. PET is a non-invasive nuclear imaging technique that is based on detection of gamma quanta emitted from the body after injection of positron-emitting radioisotope [1]. Usually, clinical PET scanners are composed of crystal detectors [2], which have two significant drawbacks: a high price and the way in which the detectors are currently aligned that does not allow for real simultaneous PET and MRI (magnetic resonance imaging) scans.

There has been a novel concept of replacing those expensive crystal scintillators with organic ones made of polymer. Due to the properties of polymers, such as low density and small atomic number of its elements, it has not been considered to be a sufficient sensor for PET detectors. Regardless of those facts, it turns out that plastic scintillators' lower efficiency can be compensated by using a large diagnostic chamber, 3D mode for image reconstruction and also by using few layers of scintillators [3]. The reduction of costs along with improved effectiveness could potentially lead to popularization of PET scanners on a larger scale.

The aim of this thesis is to experimentally evaluate the efficiency of polymer detector used in J-PET – the first PET scanner using plastic as a detection material and to check whether theoretical value of polymer scintillators' efficiency [4], matches the measured characteristics.

Chapter 2

Introduction to PET imaging technique

Positron Emission Tomography (PET) is considered an important method in imaging techniques, therefore, it is under constant development. This non-invasive technique provides metabolic assessment of tissues. Any anomalies can be detected long before anatomical or structural changes occur [5], thus PET is complementary with computational tomography (CT) or magnetic resonance imaging (MRI).

A PET scan shows glucose metabolism by creating a 3D image of the body. In order to make it possible, one is injected with radiopharmaceutical that is then distributed throughout the body. Radiopharmaceuticals are made of chemical compounds that have been altered to include an isotope and carrier molecules.

A radionuclide undergoes a β^+ decay, a process that leads to the emission of positron (e^+) in a patient's body. The general formula of a β^+ decay is:



where X and X' stand for initial and final elements, and A and Z represent mass number and atomic number, respectively, ν_e symbolizes neutrino.

Most widely used radiopharmaceutical isotope is fludeoxyglucose (FDG), which is a modified form of glucose, with attached fluorine isotope with a half-life of up to 115 minutes [6]. Due to the fact that most cancer cells have got high metabolism, the demand for glucose in the malignant tissues is higher than normal. The higher utilization of glucose results in accumulation of FDG in cancerous tissues [7]. A positron, emitted from the decay of an isotope, has got a certain kinetic energy, however, the energy decreases as it passes through the tissue. Eventually, when the kinetic energy is dissipated, the positron can annihilate. The annihilation process is a reaction of a positron with an electron (from patient's tissues) releasing, in most cases, two photons emitted in opposite directions (Figure 2.1).

Electron-positron annihilation creates two gamma quanta, each with energy of 511 keV, which is equal to rest energy of both electron and positron. The PET scanner is designed to detect these quanta.

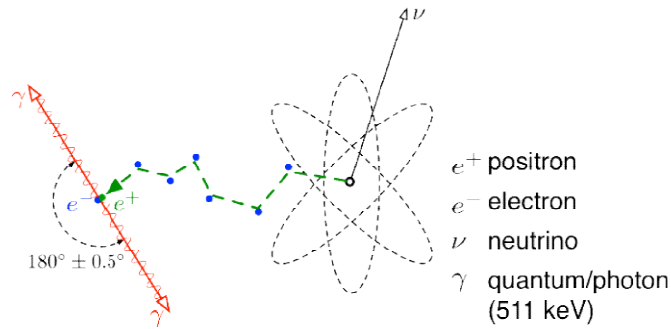


Figure 2.1: A scheme of a β^+ decay process and electron-positron annihilation. Figure adapted from [8].

It consists of detector rings which are made of many detector blocks (Figure 2.2). Each detector block is built of inorganic crystal scintillators coupled with photomultipliers. A scintillator is a substance that is capable of absorbing ionizing radiation and transforming a portion of its energy into visible light (photons), while photomultipliers are sensors which allow detection of light. Once gamma ray hits the scintillator it produces a blast of light propagating inside the scintillator, that is then registered by photomultiplier.

In order to make sure that an event is an annihilation event, both signals must exceed a defined threshold and be observed in predefined time window.

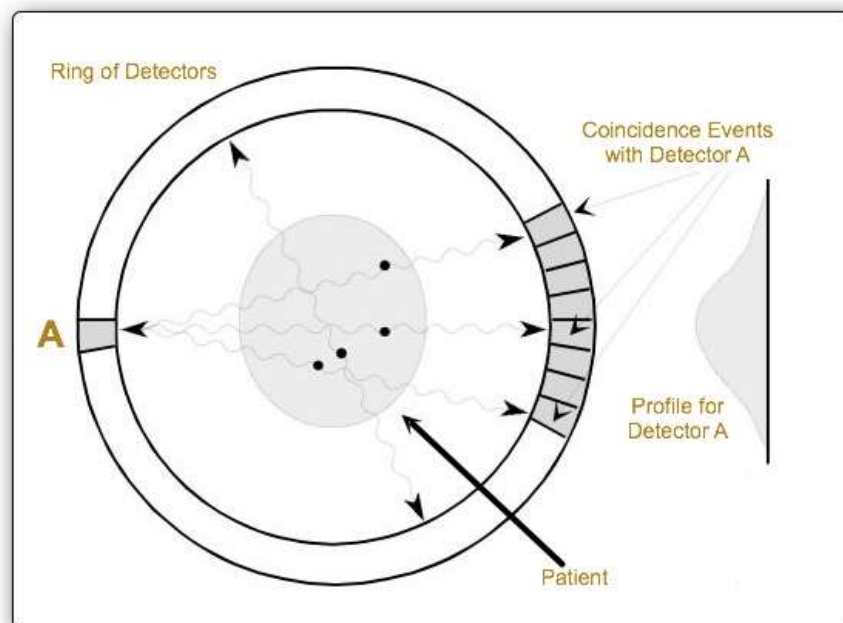


Figure 2.2: A PET Diagram. Black dots indicate places where annihilation occurred. An annihilation event candidate is created for two detectors registering signals at specific time window. Scheme presents how every detector (A) operates in coincidence with opposing detectors. Figure adapted from [9].

Coincidence event can be accredited a line, connecting two detectors that gave signal in a given time window, which is called a line of response (*LOR*). Single LOR represents a line on which an annihilation took place. A combination of LORs provides a starting point for image reconstruction.

A concept called Time-of-Flight (*TOF*) enhances quality of PET scans [10]. As mentioned before, LOR holds information of the whereabouts of annihilation, while TOF improves that information. TOF-PET method (Figure 2.3) is using time difference between two photons hitting opposite detectors to determine the line segment in which annihilation appeared [11]. This method also helps in image noise reduction.

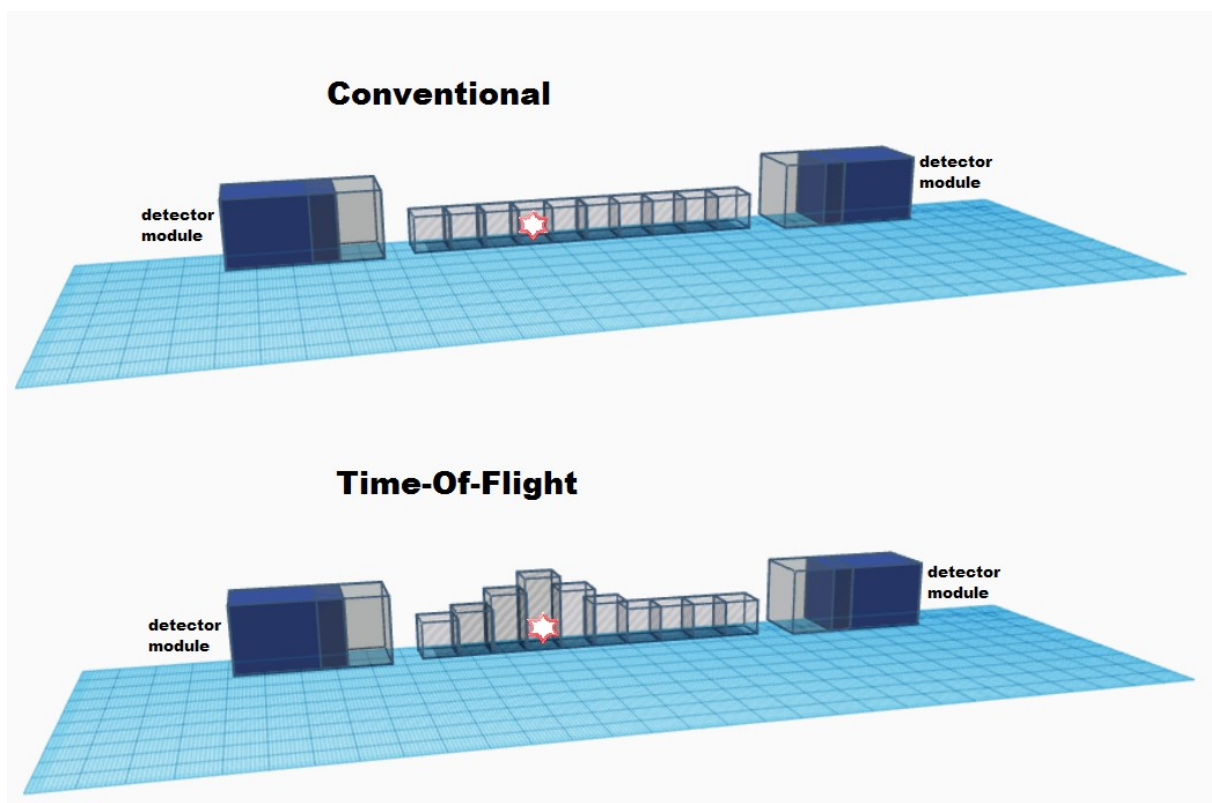


Figure 2.3: Comparison of conventional PET (no localization along LOR) and TOF-PET. Red mark indicates place where annihilation occurred. In conventional PET, time difference in photons being detected is not known, thus the probability (grey bins) of annihilation appearing in a certain place is the same along the LOR line. In TOF-PET, on the other hand, due to the measurement of difference in the detection time, it is possible to find a place where the probability of an annihilation occurrence is the highest.

Chapter 3

Polymer Scintillators as a novel approach in PET

One of the most innovative ways to improve PET scanners is to replace scintillation crystals with plastic ones. Currently, all of PET detectors are based on scintillation crystals, which are efficient when it comes to gamma ray detection, but are exceedingly costly. The idea of replacing crystal scintillators with plastic ones caused a lot of controversy due to the plastic properties. Low density and low atomic number of elements making up have a negative impact on its detection efficiency of gamma quanta. As it turns out this can be compensated. Redesigned PET scanner with organic scintillators can not only be as good as commonly used PET scanners, it can also be more economical [12].

Using plastic as a substitute for crystal has consequences in gamma ray detection. Crystal has greater density than plastic, so the probability of gamma rays interacting with its atoms is much higher. There are three main ways in which photon can interact with scintillator, that is photoelectric effect, Compton's effect and pair creation. PET scan should only detect photons that originate in annihilation, with energy of 511 keV. Effect of pair production only happens when energy of photon is either equal or greater than 1022 keV, so an annihilation photon can only transfer energy through photoelectric effect or Compton's effect.

Photoelectric effect means that a single photon transfers all of its energy to a bound electron and, consequently, the electron leaves an atom. As a result of energy conservation law and momentum conservation law, the photoelectric effect only appears for bound electrons. Compton's effect is the scattering of gamma ray (or X-ray) by either free or loosely bound electron (Figure 3.1). Loosely bound electrons have lower binding energy than the energy of photon. As a result of scattering, electron leaves an atom.

The consequence of Compton's scattering is the decline of photons energy – the wavelength of scattered photon is increased. Energy of the photon after scattering (E') on the electron of mass (m_e) depends on initial energy of a photon E and the scattering angle θ :

$$E' = E \left(1 + \frac{E}{m_e c^2 (1 - \cos \theta)} \right)^{-1}. \quad (2)$$

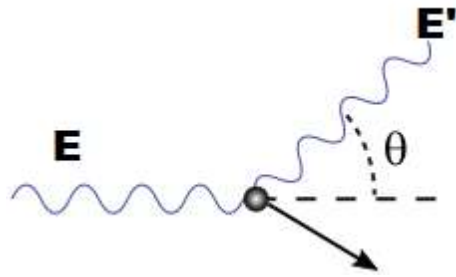


Figure 3.1: Scheme of Compton's effect. All symbols are denoted in text. Figure adapted from [13].

As previously detailed, annihilation photons interact mainly through photoelectric effect for materials with high atomic number, but interact via Compton's effect for materials with low atomic number (Figure 3.2).

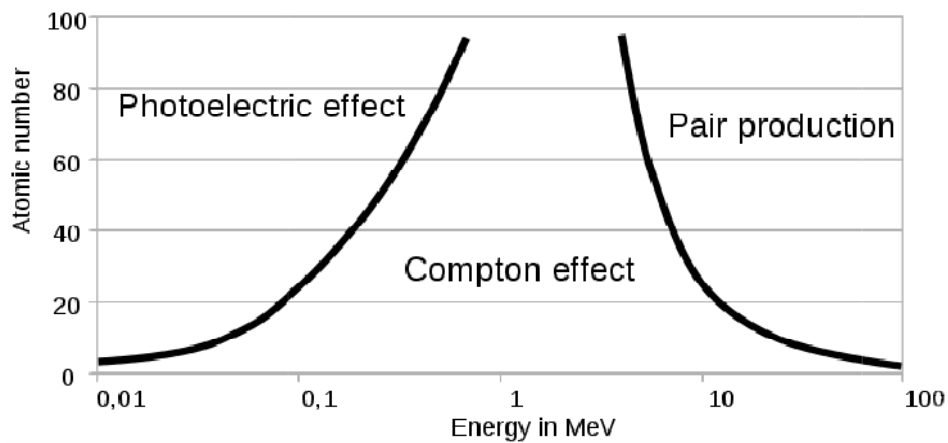


Figure 3.2: Interaction of gamma radiation with matter. Scheme presents how different types of photon interaction dominate depending on photon energy and atomic number of an absorber. Figure adapted from [14]

Polymer scintillators used in this experiment are mostly made of base polymer which is polyvinyl toluene [15]. It's a synthetic polymer composed mostly of carbon and hydrogen atoms. Small atomic number of polymer elements means that energy of photons will be transferred mainly through Compton's effect. Crystal scintillators, that are presently used, consist mainly of bismuth, caesium, germanium or thallium and other elements with high atomic numbers [2], therefore, the photoelectric effect is dominating for crystal scintillators.

Considering a Formula 2, the electron can achieve its maximum energy when gamma ray is back-scattering (scattering angle of 180°). Maximum kinetic energy that electron can gain

through Compton's scattering is equal to $2E/3$. For the energy of annihilation photon (511 keV), the maximum energy a photon can deposit is equal to 340 keV.

A PET scanner with plastic scintillators is currently being developed at Jagiellonian University [16]. Project entitled J-PET (Jagiellonian PET) focuses on the construction of PET which significantly differs from regular PET scanners. Ring of detectors has been replaced with three layers of organic detector strips arranged in cylindrical shape (Figure 3.3). Each scintillator strip has a pair of photomultipliers attached to both ends. Multiple layers increase the probability of photon detection and geometrical acceptance.

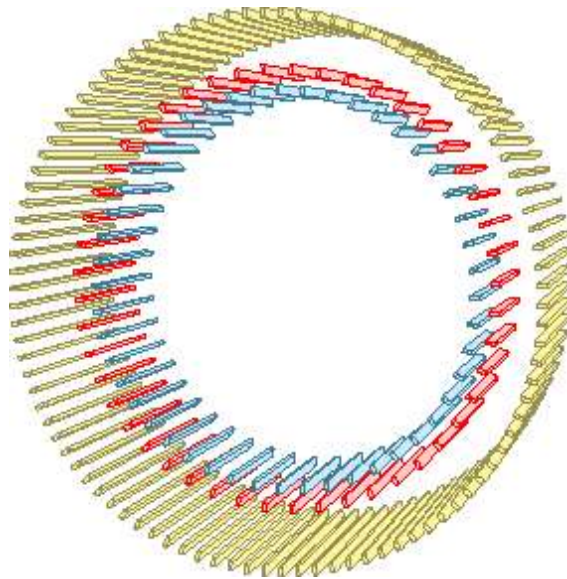
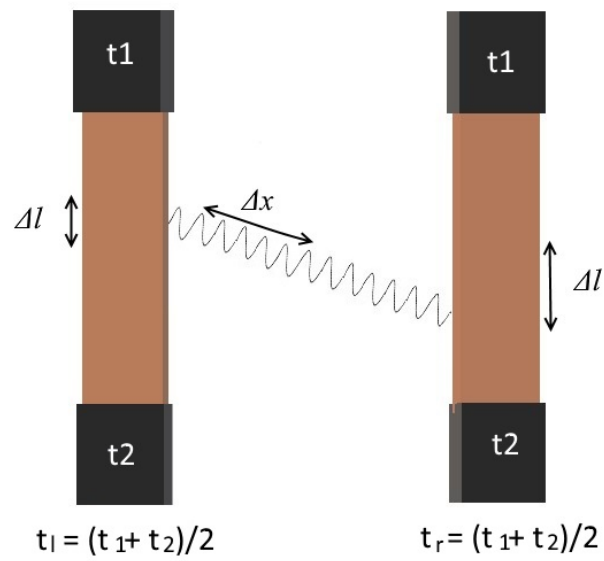


Figure 3.3: An arrangement of scintillators in J-PET. Figure adapted from [17].

Reorganized structure of detectors can reduce drawbacks caused by the properties of plastic scintillators. Long scintillators can be efficient for organic scintillators since the attenuation lengths for 511 keV gamma rays are significantly smaller for inorganic (e.g. crystal) scintillators due to the density of the used substance [2].

J-PET scanner is capable of using PET-TOF method in an extended way as a regular PET scanner would, due to the better time properties of polymers than crystals [3]. Technique itself has been modified in a way that is suitable for the new shape of detectors [17]. Exact place of gamma interaction with scintillator is registered in both plastic stripes by measuring the time difference of signals appearing in photomultipliers (Figure 3.4).



$$\Delta l = \frac{(t_2 - t_1) \cdot v}{2} \cong \frac{(t_2 - t_1) \cdot c}{4}$$

$$\Delta x = \frac{(t_l - t_r) \cdot c}{2} \Rightarrow \Delta x = \frac{\Delta t}{2} \cdot c$$

Figure 3.4: Scheme of two detector modules. Time difference measured for both ends of a scintillator strip allows for annihilation gamma hit place determination, while time difference between two strips results in annihilation place determination.

Chapter 4

Efficiency measurements

4.1. Experimental setup

Counting efficiency (ϵ) of a scintillator can be defined as a ratio of particles registered by the detector (N_{det}) to the number of all particles of this type that hit the detector (N_{hit}).

$$\epsilon = \frac{N_{\text{det}}}{N_{\text{hit}}} \quad (3)$$

Efficiency of a plastic scintillator depends on the scintillators thickness.

To designate scintillators efficiency, two crystal detectors were used along with one plastic detector. Since positron source was an isotope of sodium (^{22}Na), three detectors were needed. Sodium-22 decays emitting a positron and an excited state of Neon. Electron-positron annihilation results in two 511 keV gamma quanta emission (due to the momentum conservation, more than one photon is emitted), while Neon returns to its ground state by releasing 1274 keV gamma quanta.

Photons that originate in annihilation are emitted in the opposite directions, which is useful for the event selection. If two detectors were to face each other, and one of them would detect an annihilation gamma ray, so should the other.

The experimental setup (Figure 4.1) is based on that idea. One of the detectors is supposed to register gamma rays that come from an excited Neon passing into ground state, emitting gamma quanta of 1274 keV energy. Other 2 detectors should only register gamma quanta that come from annihilation (511 keV each). Therefore, an oscilloscope trigger is needed to detect only events useful for the determination of scintillators' efficiency.

Trigger should only be applied to the crystals detectors. If both crystal detectors detect gamma quanta, then that event will be used for further evaluation.

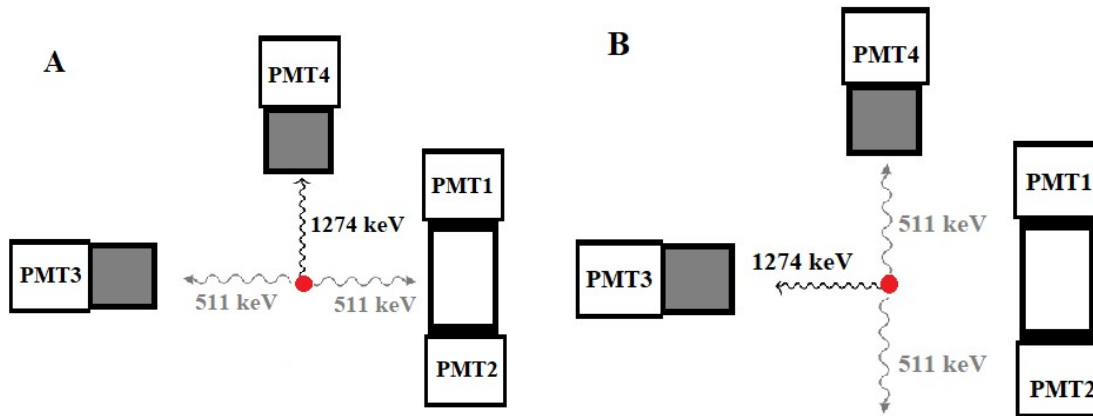


Figure 4.1: Scheme of experimental setup. Red mark indicates position of ^{22}Na source. Plastic detector module consists of plastic scintillator (white block) with two photomultipliers (PMT) coupled to both ends. Grey blocks indicate crystal scintillators. Events were registered when signal appeared in crystal scintillators coupled to PMT3 and PMT4, so both cases A and B were registered. To eliminate unwanted events, an offline discrimination of 1274 keV was applied (based on the signal charge).

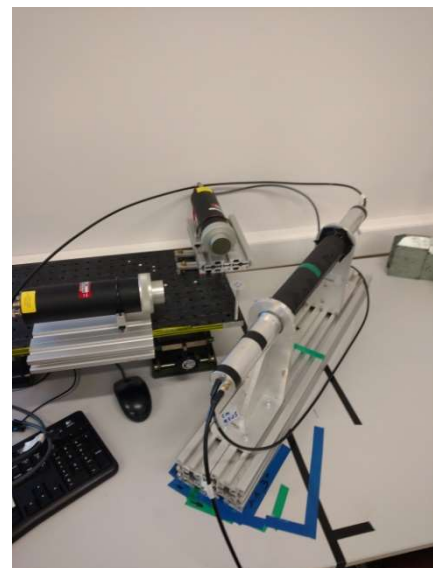
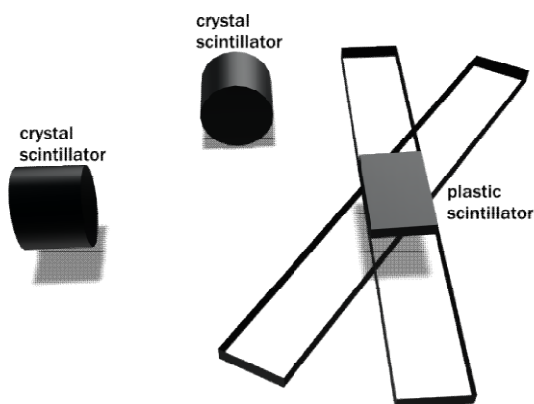


Figure 4.2: A 3D scheme of detectors. First series of measurements was conducted with short, 4 cm plastic scintillator only. After that, short scintillator was replaced with long, 30 cm plastic scintillator, which was not only placed in parallel with crystal but also rotated. After series of measurements, scintillator bottom was turned on side. A picture of an actual setup is included.

To confirm that measurements are accurate, the gain of the photomultipliers should remain unchanged for both photomultipliers coupled to crystal and plastic scintillators. In the ideal case the same range of energy (or equivalently of charge) spectra guarantee the same gain. The gain of photomultipliers strongly depends on applied voltage, therefore it can be

controlled. The same spectra can be achieved by altering the voltage accordingly. The high voltage settings used in reported measurements are presented in Table 4.1.

Table 4.1: Voltage settings established for all measurements. PMT1 and PMT2 have been coupled to the plastic scintillator, which is why the voltage is significantly lower than voltage used for photomultipliers coupled to crystal scintillators (PMT3, PMT4)

PHOTOMULTIPLIER	VOLTAGE [V]
PMT1	1320
PMT2	1220
PMT3	2300
PMT4	2460

4.2. Performed measurements

Several measurements with different geometrical settings were performed (see Figure 4.2). Five measurements with short plastic scintillator for systematic accuracy determination. Position of the centre of plastic scintillator with respect to the centre of crystal one was altered by 0.5 mm steps (Figure 4.3). The measurement for the middle position was chosen for ϵ determination. One additional measurement was performed to test the repeatability of the result by reassembling the setup and repeating the measurement.

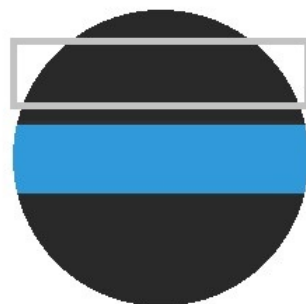


Figure 4.3: A visual representation of measurements performed for a short scintillator. In this measurement height of plastic detector module has been altered to find the best setup geometry, therefore with each step blue shape (corresponding to plastic scintillator) moved either up or down.

In order to measure ϵ for different detector thickness, a long plastic scintillator was mounted. A series of 6 measurements was conducted with 30 cm long scintillator strip. At first plastic detector module was rotated, causing the change in the scintillators thickness (depending on an angle of rotation). This measurement was conducted to examine how altering the effective length of photon interaction with scintillator would influence the counting efficiency. Angles of rotation were 0° , 27° , 36° and 44.3° . After that, 2 measurements were performed with scintillator bottom turned on the side. Angles of rotation for those 2 measurements were 0° and 44.3° .

4.3. Detectors geometry

The geometry of used detectors must be taken into consideration (Figure 4.3). Crystal detectors are cylinders facing the source with a flat, round surface with a radius of 2 cm, while plastic detector is a rectangular cuboid (5x19x300 mm). That implies that experimentally obtained value of efficiency should be calculated accordingly.

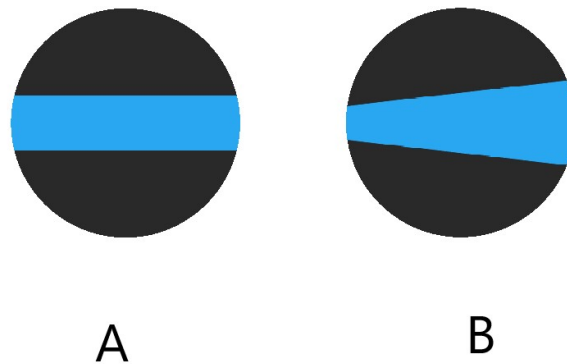


Figure 4.3: A visual representation of how differences in shapes of plastic and crystal detectors affect measurement. Supposing black shape is an intersection of crystal detector “seen” by one annihilation quantum, then the plastic scintillator “seen” by the second annihilation quantum is a rectangle. Therefore number of gamma quanta propagating towards (blue) plastic scintillator with respect to γ going towards

(black) crystal scintillator is equal to $\frac{S}{S_1}$, where S is the blue area and S_1 is the area of a circle. In some

cases one gamma ray would hit black disk, but second gamma ray would not hit blue detector, due to the difference in shapes. Image corresponds to measurement conducted with scintillator that has not been rotated in any way (A) and to measurement conducted with scintillator that has been rotated (B). The vertical length of blue shape depends on the distance between end of the plastic scintillator and crystal scintillator.

Chapter 5

Data Analysis

Registered data sample consists of signal and background events, thus energy of γ registered in detector 3 at Figure 4.1 is equal to 511 keV or 1274 keV, respectively. For each signal (voltage over time dependence) registered by a photomultiplier its charge was calculated (exemplary spectrum presented on left side of Figure 5.1). A noise was rejected by a trigger level, resulting in spectra for PMT3 and PMT4 starting from ~ 2 pC and ~ 5 pC respectively. A maximum around 0 pC (nearly overlapping PMT1 and PMT2 spectra) corresponds to events registered by crystal scintillators but not by plastic one. In order to reject background events an offline cut on PMT4 was introduced.

Accepting only events with charge greater than 8 pC at PMT4, results in registering only 1274 keV gamma quanta in this detector, as a consequence 511 keV gamma quanta are registered in PMT3 (N_{hit}). To obtain N_{det} (see Equation 3) a cut on the charge on PMT 1 and 2 was also applied. Range of spectra for each pair of detectors: plastic (1 and 2) and crystal (3 and 4) is not the same, because of the gain misscalibration, however this effect is corrected by applying different cut values for detectors 1 and 2.

Events with charge greater than the cut value corresponds to events registered in plastic scintillator (N_{det}). Due to the effect described in Section 4.3, the number of not registered events must be decreased by S/S_1 factor (see Table 5.1).

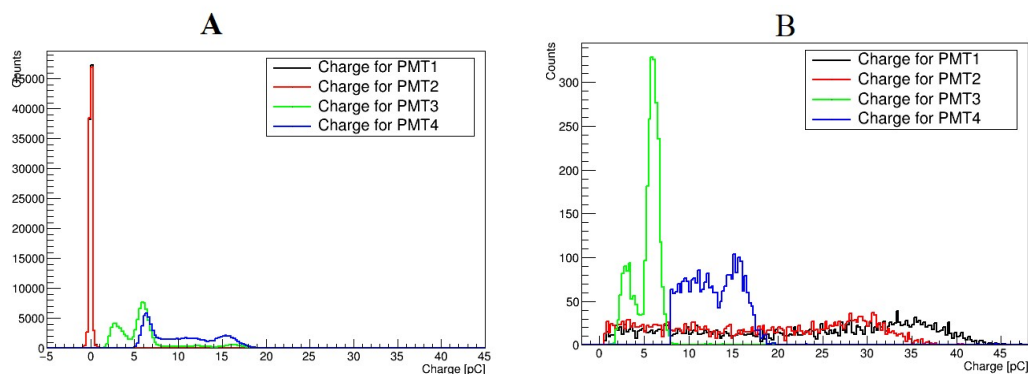


Figure 5.1: Charge spectra collected in a measurement. Charge is proportional to the energy of gamma quanta. For charge spectra from PMT 3 and PMT 4, both Compton's edge and photoelectric peak are visible for 511 keV (~ 6 pC) and 1274 keV (~ 15.5 pC) quanta. For charge spectra from PMT 1 and PMT 2 only Compton's edge is visible (signals from plastic detectors). Diagrams present the same data set before applying cuts on charge (A) and after (B). The vertical scale differs.

Measurement number	Scintillator length [cm]	Scintillator thickness [mm]	S/S ₁ factor
1	4	19.0	0.34
2	4	19.0	0.32
3	4	19.0	0.33
4	4	19.0	0.32
5	4	19.0	0.34
6	4	19.0	0.33
7	30	19.0	0.33
8	30	26.6	0.32
9	30	23.5	0.32
10	30	21.3	0.32
11	30	5.0	1
12	30	7.0	0.81

Table 5.1: The factor of S/S₁, which indicates the ratio of gamma quanta that did not hit the plastic scintillator due to the geometry of used detectors. The ratio maintains the same level for short scintillator, which was not rotated, but instead was moved upwards and downwards. The ratio remained stable for long rotated scintillator, but peaked when scintillator was turned to the side (measurements 11 and 12).

When evaluating efficiency, a certain cut on PMT1 and PMT2 signals must be applied, as mentioned in the previous paragraph. A simulation of detectors efficiency as a function of detector thickness can be plotted both with and without on energy cut [4], but an experimental approach requires applying a cut.

Due to the attenuation length, quantum efficiency and cut used, an adequate correction is needed to calculate the efficiency. If a particle hits the detector and deposits E_0 energy within the detector, then owing to attenuation length an energy of E_1 ($E_1 < E_0$), will reach photomultiplier.

Light attenuates in plastic, due to photon absorption or scattering. Attenuation depends on the size of material, bulk attenuation length provided by manufacturer is 110 cm for plastic scintillators used in a long sheet [15]. Attenuation lengths, experimentally evaluated (for cross-section of 5 x 19 mm as for J-PET detector) allow one to calculate the percent of light that will not reach the photomultiplier due to the scattering or absorption [18].

Assuming that gamma quanta interacts in a centre of a scintillator, energy losses of propagating light due to attenuation are equal. Once the place of interaction is near scintillators end, energy losses change significantly, therefore number of photons reaching

photomultipliers is no longer equal. Photomultiplier outputs an electrical charge that is proportional to light intensity, thus different number of photons results in different charge values [18]. Energy attenuation is given by the general formula:

$$E_1 = E_0 e^{-\frac{x}{\lambda}}, \quad (4)$$

where E_0 is the initial energy, E_1 is the energy of light after propagation by distance x and λ is the attenuation length.

Due to the geometrical limits of used scintillator, the Formula 4 should be extended to two exponents as in Ref. [18]. In the reported measurements, the average mean of parameters from Ref. [18] was used:

$$E_1 = E_0 (\bar{c}_1 \cdot e^{-\frac{x}{\bar{\lambda}_1}} + \bar{c}_2 \cdot e^{-\frac{x}{\bar{\lambda}_2}}), \quad (5)$$

where $\bar{c}_1 = 0.692 \pm 0.042$, $\bar{c}_2 = 0.168 \pm 0.018$, $\bar{\lambda}_1 = 372 \pm 4$ [mm], $\bar{\lambda}_2 = 10 \pm 2$ [mm].

The obtained result should be corrected by $Att^2 = \left(\frac{E_1}{E_0}\right)^2$ factor, which is raised to the power of 2, because the presence of signals at both ends of plastic scintillator was required.

Apart from light attenuation, quantum efficiency of a photocathode in a photomultiplier can also affect the measurement. Quantum efficiency can be defined as a ratio of photoelectrons produced to the number of photons that have been absorbed. The quantum efficiency (Q_{eff}) of used photomultipliers (Hamamatsu R9800) is 25% [19]. Plastic was coupled to two photomultipliers and for that reason a correction of $Q_{eff}^2 = 6\%$ was applied.

Once light of energy E_1 reaches the photomultiplier, E_2 ($E_2 < E_1$) will be registered due to the quantum efficiency. The cut applied to the photomultipliers will separate events, so that the only analysed signals have the energy greater than cut value.

Energy corresponds to charge hence the maximum of deposited energy $E_{max} = 340$ keV is proportional to some charge C_{max} (that cannot be experimentally evaluated), the experimental value is C_{max}^{exp} ($C_{max} > C_{max}^{exp}$). Similarly, the energy cut (E_{cut}) is proportional to the charge

cut (C_{cut}), yet value of the charge cut will depend on experimental charge cut (C_{cut}^{exp}), quantum efficiency and light attenuation, with a formula:

$$C_{cut}^{exp} \cdot Q_{eff}^2 \cdot Att^2 = C_{cut} \quad (6)$$

Assuming linear dependence between energy and charge, the value of charge cut to be applied in this analysis, which would correspond to the reference energy cut of 100 keV as in Ref. [4] is given as:

$$C_{cut}^{exp} = \frac{E_{cut} \cdot C_{max}^{exp}}{E_{max}} \quad (7)$$

Data acquired after energy cuts could be used to designate scintillators efficiency if plastic and crystal detector were the same size. Difference in shape (Figure 4.3) can be compensated by introducing a ratio of area of plastic detector to the area of crystal detector (see S/S_1 ratio in Sec. 4.3). Using that ratio in the efficiency calculation will correct the discrepancy in shapes of the detectors. Differences in the shapes of the detectors were significant and therefore calculating the ratio of detector shapes was a necessity.

Therefore final formula for counting efficiency is:

$$\varepsilon = \frac{A}{A + B \frac{S}{S_1}} \quad (8)$$

where A stands for the number of events registered by plastic detector (N_{hit}), B stands for the number of events registered by a crystal detector only (not registered by plastic detector), S/S_1 is the size ratio of detectors used.

To evaluate how detector thickness affects the efficiency, long plastic scintillator has been rotated. Greater angle of rotation meant greater thickness, but due to the turn distances between two detectors would change as presented on Figure 4.3 (B).

Chapter 6

Results and Conclusions

The measurements conducted with short scintillator strip for systematic accuracy determination (measurements 1-6, Table 5.1) are presented in the Figure 6.1. The vertical position of plastic scintillator was changed for each of the measurements by 0.5 mm, therefore the measured values differ. As systematical error due to geometrical misalignment the difference between measurement X and Y was used resulting in $\sigma_{syst}^{geom} = 0.016$.

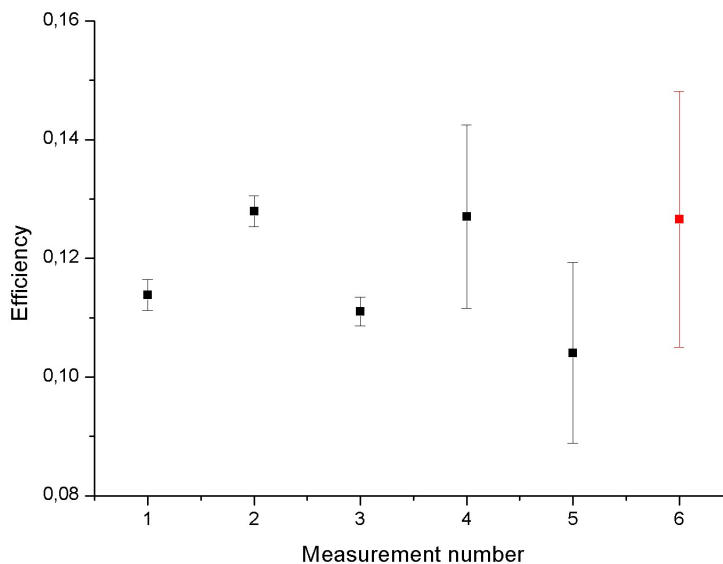


Figure 6.1: Efficiency obtained for measurements 1-6. Short scintillator was used, therefore the thickness remained the same. For measurements 1-5 the vertical position of plastic detector was altered by 0.5 mm per measurement (1 – lowest position, 3 – central, 6 – highest). Measurement 6 was conducted to prove the repeatability of the results. Measurements 4-6 lasted longer than measurements 1-3, therefore are less accurate.

For each measurement listed in Table 5.1 the efficiency was calculated using Formula 8 for data with cut defined by Equation 7. Uncertainty of the counting efficiency has been calculated using the exact differential method. The systematic contribution are obtained by changing values used in the analysis by 1σ separately and then calculating the efficiency

once more. The results are listed in Table 6.1. The total systematic uncertainty is calculated

$$\text{as: } \sigma_{\text{syst.}}^{\text{total}} = \sqrt{\sum_i^n \sigma_i^2}.$$

The Figure 6.2 shows the final efficiency determination as a function of detector thickness,

$$\text{where error bars are calculated as } \sigma_{\text{total}} = \sqrt{\sigma_{\text{stat.}}^2 + \sigma_{\text{syst.}}^2}.$$

The function:

$$\varepsilon(x) = A(1 - e^{-Bx}), \quad (9)$$

was fit to the data points, resulting in parameter values: $A_{\text{exp}} = 0.188 \pm 0.052$ and $B_{\text{exp}} = 0.47 \pm 0.26 \text{ [cm}^{-1}\text{]}$, while based on approach described in Ref. [4], the theoretical values are: $A_{\text{theo}} = 0.693$, $B_{\text{theo}} = 0.10 \text{ [cm}^{-1}\text{]}$ (with negligible error). Although the obtained parameters values are not within error bars, the efficiency for 1.9 cm confirms assumptions used to motivate construction of the J-PET system with plastic scintillators. The assumed efficiency is compensated by additional detection layers and bigger field of view with respect to standard PET devices.

i	Parameter	Parameter accuracy	σ_{syst}
1.	Q_{eff}	$\pm 2\%$	0.019
2.	Att	$C_1 = 0.042$ $C_2 = 0.019$ $\lambda_1 = 4 \text{ [mm]}$ $\lambda_2 = 2 \text{ [mm]}$	0.014
3.	<i>Setup geometry</i>	1 mm	0.017
4.	<i>Setup reassembly</i>	-	0.016

Table 6.1: Systematic uncertainties of measurements. For measurements performed with long scintillator all of parameters were used in calculations. For measurements performed with short scintillator attenuation effect was neglected in calculation.

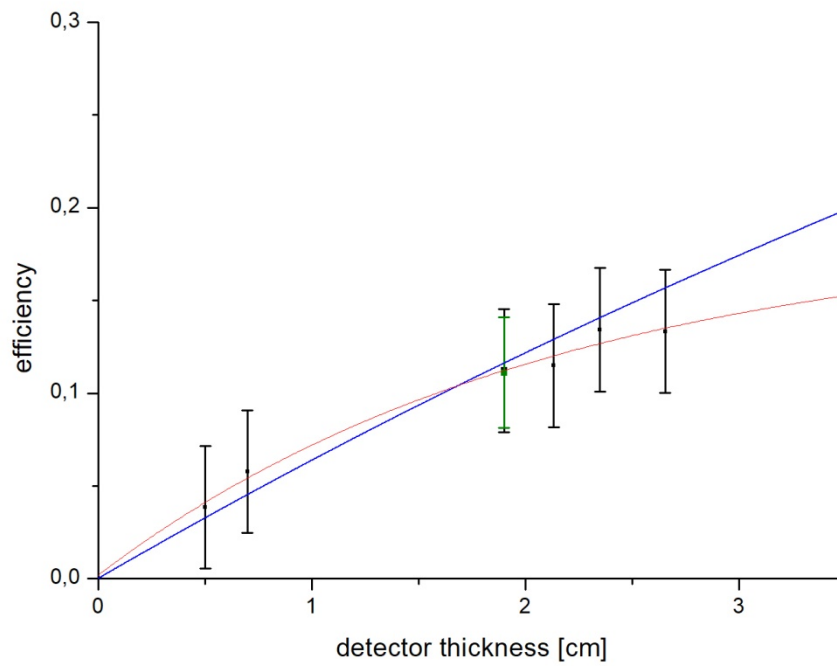


Figure 6.2: Comparison of the theoretical predictions, based on Equation 9 and parameters given in text (blue) and experimental results (red). Black points are experimentally obtained values for the long scintillator, while green point (for 1.9 cm thickness) corresponds to the short scintillator, with attenuation length effect neglected.

Acknowledgements

I would like to express my gratitude to my supervisor Dr Eryk Czerwiński for the guidance, patience in answering questions and time spent in preparation of this thesis.

I would also like to show appreciation to Prof. Paweł Moskal for the given opportunity to work in the J-PET group.

Furthermore, I am grateful to Szymon Niedźwiecki for the help and advice with data analysis and programs used for it.

I would also like to acknowledge Aleksander Gajos as the author of program used for data analysis.

Bibliography

- [1] Valk, P.E. et al., eds. Positron Emission Tomography. Basic Science and Clinical Practice. 2003, Springer: Heidelberg
- [2] Humm, J. et al. "From PET detectors to PET scanners." *European journal of nuclear medicine and molecular imaging* 30.11 (2003): 1574-1597.
- [3] Moskal, P. et al. "TOF-PET detector concept based on organic scintillators." *Nucl Med Rev* 15 (2012): C81.
- [4] Niedźwiecki, S., *Studies of detection of γ radiation with use of organic scintillator detectors in view of positron emission tomography*, master thesis (2011), Jagiellonian University
- [5] Zhu, A. et al. "Metabolic Positron Emission Tomography Imaging in Cancer Detection and Therapy Response" *Seminars in Oncology*, Volume 38, Issue 1, 55 – 69
- [6] Yu, S. "Review of ^{18}F -FDG synthesis and quality control." *Biomed Imaging Interv J* 2.4 (2006): e57
- [7] Lindholm, P. et al. "Influence of the blood glucose concentration on FDG uptake in cancer—a PET study." *Journal of nuclear medicine* 34.1 (1993): 1-6.
- [8] Maus, J. "Annihilation" (<http://jens-maus.de/>) [Public domain], via Wikimedia Commons
- [9] Maher, K. "A PET diagram" using OmniGraffle.
<http://en.wikibooks.org/wiki/File:PetDiag2.jpg> [Public domain], via Wikimedia Commons
- [10] Karp, J. et al. "Benefit of time-of-flight in PET: experimental and clinical results." *Journal of Nuclear Medicine* 49.3 (2008): 462-470.
- [11] Karp, J. et al. "Time-of-flight PET." *PET Center of Excellence Newsletter* (2006).
- [12] Moskal, P. et al. "J-PET: nowy Pozytonowy Emisyjny Tomograf zbudowany z plastikowych detektorów", *Inzynier i Fizyk Medyczny* 4 (2015) 235
- [13] Jabber, W., English language Wikipedia, CC-BY-SA-3.0, via Wikimedia Commons
- [14] von Berklas (Eigenes Werk) CC BY-SA 3.0 oder GFDL, via Wikimedia Commons

- [15] Plastic Scintillation Material Data Sheets: BC-418, BC-420, BC-422. 2017. *Saint-Gobain Crystals*. [ONLINE] Available at: www.crystals.saint-gobain.com. [Accessed August 2016]
- [16] Moskal, P.: "Strip device and the method for the determination of the place and response time of the gamma quanta and the application of the device for the Positron Emission Tomography". Patent Application No. P 388 555 [WIPO ST 10/C PL388555], 2009.
- [17] Moskal, P. Et al. "Strip-PET: a novel detector concept for the TOF-PET scanner." *Nuclear Medicine Review* 2012.15 Suppl C (2012): C68-C69.
- [18] Bednarski, T. "Kalibracja energetyczna i synchronizacja czasowa modułarnego scyntylacyjnego systemu detekcyjnego do tomografii TOF-PET."
- [19] Photomultiplier tube R9800. 2017 *Hamamatsu*. [ONLINE] Available at: <http://www.hamamatsu.com/us/en/index.html>. [Accessed July 2017]